


Testing the nonclassicality of gravity with the field of a single delocalized mass

Alessandro Pesci^{1,*} and Pierbiagio Pieri^{2,1,†}¹*INFN, Sezione di Bologna, Via Irnerio 46, 40126 Bologna, Italy*²*Dipartimento di Fisica e Astronomia, Università di Bologna, Via Irnerio 46, 40126 Bologna, Italy*
 (Received 27 July 2023; revised 12 October 2023; accepted 15 November 2023; published 1 December 2023)

Most of the existing proposals for laboratory tests of a quantum nature of gravity are based on the use of two delocalized masses or harmonically bound masses prepared in pure quantum states with large enough spatial extent. Here a setup is proposed that is based on a single delocalized mass coupled to a harmonically trapped test mass (undergoing first expansion and then compression) that moves under the action of gravity. We investigate the in-principle feasibility of such an experiment, which turns out to crucially depend on the ability to tame Casimir-Polder forces. We thus proceed with a design aimed at achieving this, trying at the same time to take advantage of these forces rather than only fighting them.

DOI: [10.1103/PhysRevA.108.062801](https://doi.org/10.1103/PhysRevA.108.062801)

I. INTRODUCTION

No direct proof exists so far of the quantum nature of the gravitational field. The smallness of the Planck length l_P , at whose scale the quantum aspects of gravity should unavoidably appear, has always been a formidable obstacle to any attempt to check for such quantum features at laboratory scales. This might be about to change, however, due to the prodigious progress accumulated over the years in sensing and controlling quantum systems, as well as to some new twists [1,2].

The basic idea, which dates back at least to an observation by Feynman [3], is to look at the gravitational field sourced by a quantum system in a superposition of states, prototypically corresponding to spatially separated states. The effects on a test mass at a distance from the source should depend on the nature of the field. If the gravitational field is quantum, the test mass should experience a superposition of field states, each state leading to a different time evolution of the test mass, with a building up of entanglement between test and source masses during this evolution. If the field is classical, it is single valued and no entangling with the source mass is possible. This is, e.g., the case of gravity in the semiclassical approximation [4,5], in which the source is quantum and the field is classical, with the field experienced by the test mass corresponding to the expectation value of the energy-momentum tensor over the quantum state of the source.

Two contrasting requirements apply in general to quantum gravity experiments. On one hand, large masses are desired to produce large gravitational fields and thus amplify the signal to be measured. On the other hand, the larger the mass is, the more difficult it is to control quantum decoherence by the environment [6]. As a matter of fact, there is still a huge gap [7] between the largest masses for which an exquisite quantum

control of the position has been attained (approximately equal to 10^{-16} kg [8]) and the smallest masses whose gravitational fields have been directly measured (approximately equal to 10^{-4} kg [9]). As a consequence, even just revealing the quantum nature of the source by the classical gravitational field it produces, as in the semiclassical approximation, is still something far in the future (see [7] for an explicit proposal in this respect).

In view of this situation, many configurations have been proposed that allow for an increase in the sensitivity to possible quantum gravitational effects [10–13], invariably involving, however, masses somewhat larger than what is granted by present limitations on quantum control. Recently, a very promising new twist has been given by methods in which the information on the effects of the gravitational field is encoded in the variations of the quantum-mechanical phase of two quantum systems coupled only by gravity, each system being in a superposition of states (an early description of these methods was given in [14] and subsequently published in [15]). These ideas have been applied to pairs of delocalized particles, as in [15,16], or to pairs of quantum harmonic oscillators, as in [8,17,18].) The evolution of the quantum phase, driven by the gravitational field sourced by the masses, would lead to the creation of detectable entanglement if the field is treated as quantum. This is an example of a general strategy for any realistic attempt at evidencing the quantum nature of gravity in a laboratory: Focus on verifying features that cannot be explained in a classical setting rather than searching for $O(\hbar)$ corrections to classical results (which would be invariably too small, given the smallness of the Planck length l_P) [19]. In the above proposals, masses greater than approximately 10^{-15} – 10^{-14} kg have been considered.

In addition, methods that do not require the occurrence of entanglement have been proposed. One example is based on the detection of non-Gaussianity in Bose-Einstein condensates [20]. A second recent proposal is instead based on the measurement of a properly defined classical simulation fidelity between the actual state of a gravitationally interacting

*pesci@bo.infn.it

†pierbiagio.pieri@unibo.it

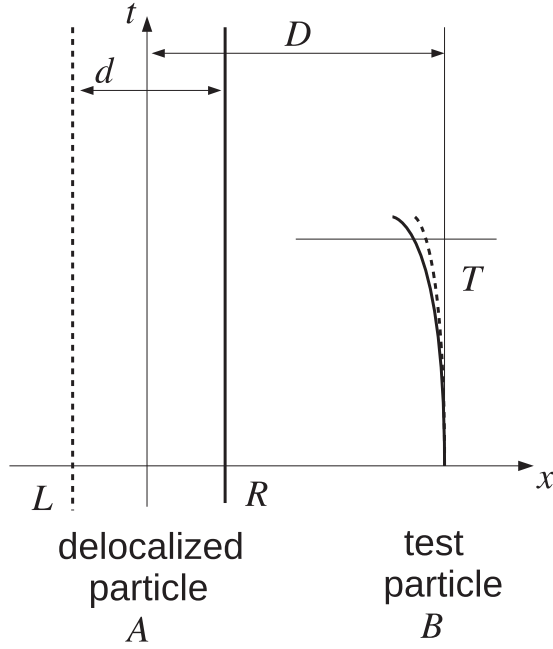


FIG. 1. Basic conceptual scheme for the investigation of the quantum nature of the gravitational field. A test particle B probes the field sourced by a particle A that is in a state delocalized between L and R , assuming the field is entangled with the superposed locations.

system undergoing a time evolution and the expected time-evolved state if the gravitational field were quantum [21].

A difficulty in most of these methods [8,15–18] is the need to have complete control of the evolution of two spatially delocalized or spatially extended wave packets against environmental decoherence [6]. Furthermore, a general issue in essentially all proposals [8,15–18,21] is the presence of Casimir-Polder forces [22–24] which become dominant over gravitational effects at small distances, severely constraining how close to the source one can probe the field, thus limiting the intensity of the gravitational effects one is looking for. Taking advantage of some recent ideas [9,25,26] on how to attenuate Casimir-Polder effects, the aim of the present paper is to reconsider the case of a single delocalized particle and propose a configuration that seems in principle able to discriminate between a classical and a quantum description of the gravitational field.

II. ENTANGLING GRAVITATIONAL FIELD

The basic idea behind the investigation of the quantum nature of the gravitational field can be illustrated as follows. A particle A , with mass m_A , is prepared with its center of mass in a superposition of states spatially separated by a distance d . The test particle B with mass m_B is placed at a distance D from A (see Fig. 1). At time $t = 0$ the trapping potential that keeps the particle B localized is switched off so that B is free to move in the field sourced by A . After a time T , the position of B is measured. The outcome will be different if the gravitational field is quantum or classical.

If the field is quantum, at $t = 0$ the system $A\Phi B$, formed by the two particles A and B and the field Φ sourced by A , is in a product state between subsystems $A\Phi$ and B . It is however

entangled within the subsystem $A\Phi$,

$$|\psi(0)\rangle = \frac{1}{\sqrt{2}}(|x_L^A\rangle|\phi_L\rangle + |x_R^A\rangle|\phi_R\rangle)|x^B(0)\rangle \quad (1)$$

(here the subscripts label the branch that sources the field).

Assuming no effects from the environment, at time t the two branches evolve to

$$\begin{aligned} |x_L^A\rangle|\phi_L\rangle|x^B(0)\rangle &\rightarrow |x_L^A\rangle|\phi_L\rangle|x_{\phi_L}^B(t)\rangle, \\ |x_R^A\rangle|\phi_R\rangle|x^B(0)\rangle &\rightarrow |x_R^A\rangle|\phi_R\rangle|x_{\phi_R}^B(t)\rangle, \end{aligned} \quad (2)$$

with $x_{\phi_L}^B(t)$ and $x_{\phi_R}^B(t)$ the evolution of B in the fields ϕ_L and ϕ_R , respectively. One thus has

$$|\psi(t)\rangle = \frac{1}{\sqrt{2}}[|x_L^A\rangle|\phi_L\rangle|x_{\phi_L}^B(t)\rangle + |x_R^A\rangle|\phi_R\rangle|x_{\phi_R}^B(t)\rangle], \quad (3)$$

with entanglement between $A\Phi$ and B and with $|x_{\phi_L}^B(0)\rangle = |x_{\phi_R}^B(0)\rangle = |x^B(0)\rangle$. After a certain time T , the states $|x_{\phi_L}^B(t)\rangle$ and $|x_{\phi_R}^B(t)\rangle$ will correspond to wave packets sufficiently apart in space to be in practice orthogonal to each other.

If, on the contrary, the field is classical and is sourced by the expectation value $\langle T_{ab} \rangle$ of the energy-momentum tensor, at $t = 0$ one has

$$|\psi(0)\rangle = \frac{1}{\sqrt{2}}(|x_L^A\rangle + |x_R^A\rangle)|x^B(0)\rangle. \quad (4)$$

Now B is under the influence of the field $\phi = \phi(\langle T_{ab} \rangle)$, yielding

$$|\psi(t)\rangle = \frac{1}{\sqrt{2}}(|x_L^A\rangle + |x_R^A\rangle)|x^B(t)\rangle, \quad (5)$$

with B not discriminating the branch of A , thus remaining unentangled for all times t .

It is crucial to have some flavor of the displacements one can have for the test particle in the two branches. An informal estimate can be obtained as follows. First of all, we note that the configuration displayed in Fig. 1 is not optimal since the displacements at time T of B from the initial position $x^B(0)$ are in the same direction (towards A) for both L and R branches (and in the classical field case as well). The separation Δx between the displacements for the two branches is thus proportional to the absolute value of the difference of the (nearly equal and weak) fields in the two branches. A much better configuration is obtained by placing B between the superposed positions as in Fig. 2; in this case Δx is proportional to the sum of the absolute values of the fields.

As already mentioned, one has to fight against Casimir-Polder forces (more on this later). A distance $l_{CP} \approx 160 \mu\text{m}$ guarantees (for silica masses, independently of their size) that the ratio $E_{CP}/E_G < 0.1$, where E_{CP} and E_G are the Casimir-Polder and gravity potential energies, respectively. Choosing $d/2 = l_{CP}$, one gets $\bar{x} \equiv \frac{\Delta x}{2} = \frac{1}{2}a_x T^2 = 2\frac{Gm_A}{d^2}T^2$, where a_x is the acceleration of B and G is Newton's constant. For the (quite optimistic) values $m_A = 10^{-11} \text{ kg}$ and $T = 1 \text{ s}$ one obtains $\bar{x} = 1.3 \times 10^{-14} \text{ m}$.

Comparing this value of \bar{x} with the spread σ_x achievable for masses cooled to the ground state in an optical tweezer [27–29], $\sigma_x \approx 0.1\text{--}1 \text{ pm}$ [8], one sees that we are far from the required sensitivity. This is mainly due to the large distances involved to reduce the importance of Casimir-Polder forces

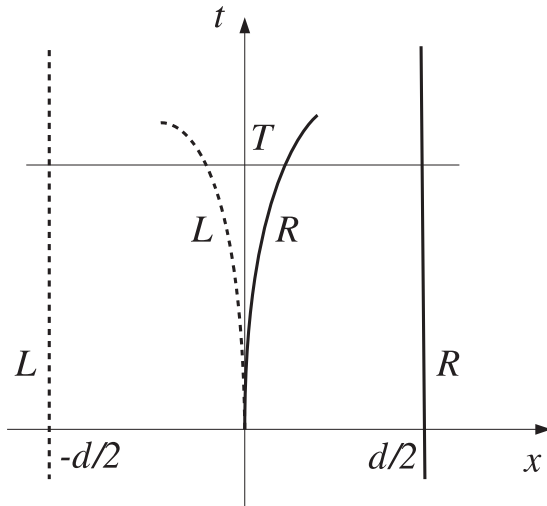


FIG. 2. Same as in Fig. 1 but with an improved configuration to enhance the displacement of the test particle.

(for the assumed mass and evolution time). This is in spite of having been very generous with our assumptions on technical capabilities. We have indeed taken quite a large value for the delocalized mass and the most convenient geometric configuration to enhance the displacement (this resulting, however, in uncomfortably large separations between the two states of the delocalized mass; cf. [6]). We have also assumed that the state superposition can be kept even with the test particle placed between L and R and for an evolution time T which is very long compared to typical decoherence times (and which requires a high control of the displacements due to free fall).

This indicates that in order to have any chance to probe the quantum nature of gravity along the above lines, one should first find a way to overcome the limitations imposed by Casimir-Polder interactions. A description of how this might be attempted is the aim of the following sections.

III. TAMING (AND EXPLOITING) THE CASIMIR-POLDER FORCES

The aim of this section is to describe ways to circumvent the issues posed by Casimir-Polder forces. We will see that setups can be considered not only in which this looks possible, but which also allow one to benefit from these forces rather than simply fighting them (somewhat similarly to Ref. [30], which contemplated the possibility to use the Casimir force to strongly couple an ancillary system to gravitationally interacting masses).

The first step in this direction is the observation that Casimir-Polder forces can be conveniently screened by using conducting plates. This was indeed used in [9] to allow masses to be close enough to each other to make detection of their gravitational field possible. Screening with conducting plates was also proposed in [25,26] as a modification of the proposal [15,16] aiming at revealing gravitational entanglement between two delocalized particles close to each other. Indeed, the insertion of a perfectly conducting plate between the delocalized particles allows one to screen the Casimir-Polder force between the particles, replacing it with the force between each particle and the plate, of the same nature but of lower strength.

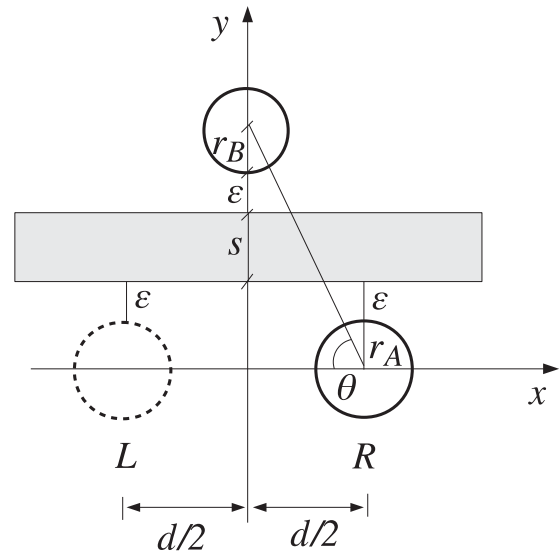


FIG. 3. Configuration with a horizontal metallic plate shielding the Casimir-Polder forces between test and source masses, helping, at the same time, the levitation of the (heavier) delocalized particle A .

This allows one to reach smaller distances between particles (roughly from the $160\ \mu\text{m}$ mentioned before to approximately $40\text{--}50\ \mu\text{m}$ [25,26]), thus enhancing the gravitational effects and allowing for milder requirements for the required separation d between the superposed positions.

In the setup of Fig. 1 one could benefit from this screening by inserting a conducting plate between A and B . However, in view of the drawbacks of this configuration discussed above, only a marginal gain could be reached in this case.

It is not immediately clear how to use this screening for the more promising setup of Fig. 2. Indeed, it looks that one has to introduce two conducting plates, placed symmetrically on the two sides of the test particle in order to separate it from the two possible positions of the delocalized source particle. This is clearly a problem, since it is not at all obvious how a delocalized state could be prepared in the presence of conducting plates between the two superposed positions.

A more convenient arrangement is shown in Fig. 3. In it, a single conducting plate screens the Casimir-Polder forces between the two particles. In addition, the Casimir-Polder force between the plate and the delocalized particle acts in the same way for the two superposed positions. In this way, the coherence of the delocalized state is not affected. Finally, the Casimir-Polder force by the plate on the test particle is in the direction orthogonal to the plate and thus does not produce displacements parallel to the plate, which are the ones relevant to detect the gravitational effects we are after. The same considerations apply to the gravitational forces between test and source masses and the plate. As a matter of fact, irregularities on the surfaces such as random patch potentials and density fluctuations in the materials could possibly affect both the coherence of the delocalized state and the displacements of the test particle. We will return to this issue later on, when focusing on Casimir-Polder effects.

Taking the x axis in the direction connecting the two superposed positions L and R , the displacement \tilde{x} induced along x

by A in branch $|x_R\rangle$ can be estimated as $\tilde{x} = \frac{1}{2}a_x T^2$, with

$$a_x = \frac{Gm_A}{(d/2)^2 + y_B^2} \cos \theta \quad (6)$$

$$= \frac{Gm_A}{(d/2)^2 + y_B^2} \frac{d/2}{[(d/2)^2 + y_B^2]^{1/2}} \quad (7)$$

$$= \frac{2}{3\sqrt{3}} \frac{Gm_A}{y_B^2}, \quad (8)$$

where $y_B = r_A + 2\epsilon + s + r_B$ (see Fig. 3). To get Eq. (8) we used the most favorable geometric conditions for given y_B , namely, the value of $d/2$ that gives the largest x component F_x of the gravitational force between A and B , corresponding to $d/2 = y_B/\sqrt{2}$.

By taking $T = 1$ s, $m_A = 10^{-11}$ kg, $m_B = 10^{-14}$ kg (corresponding to $r_A = 9.7$ μm and $r_B = 0.97$ μm , respectively, for silica), $\epsilon = 1$ μm , and $s = 1$ μm , the optimal separation turns out to be just $d \approx 2r_A = 19.4$ μm , with a resulting value for $\tilde{x} \approx 0.7$ pm that is right within the range we mentioned above as reasonably reachable with optical tweezers. For $m_A < 10^{-11}$ kg, the optimal separation d is within $2r_A < d < 19.4$ μm .

In the above estimate we have considered $m_B = 10^{-14}$ kg. This value is about 50 times the heaviest masses that at present can be harmonically controlled and cooled to the ground state (which are made of about 10^{11} nucleons [29,31], corresponding to approximately 2×10^{-16} kg). The spread of x_B in the ground state is

$$\sigma_x = \sqrt{\frac{\hbar}{2m_B\omega}}, \quad (9)$$

with ω ($\sim 2\pi \times 100$ kHz [29,31]) the angular frequency of the trapping potential. For $m_B = 10^{-14}$ kg, Eq. (9) gives $\sigma_x = 0.09$ pm, and the \tilde{x} we have just obtained appears definitely detectable.

Here we are assuming that the spread $\sigma_x(T)$ in the position of B after a time T is the same as the initial one, which is determined by Eq. (9). One might wonder if this assumption is justified. Indeed, the initial momentum spread $\sigma_p(0)$ implies that after a time t one has $\sigma_x^2(t) = \sigma_x^2(0) + \sigma_p^2(0) \frac{t^2}{m^2}$ (see, e.g., [32]), with $\sigma_p(0) \geq \frac{\hbar}{2\sigma_x(0)}$. For $t > 0$, this implies $\sigma_x^2(t) > \hbar t/m$ [33] (corresponding to the standard quantum limit; see, e.g., [34]). Using $t = 1$ s and $m = 10^{-14}$ kg, one obtains $\sigma_x(1 \text{ s}) > 10^{-11}$ m, which is about two orders of magnitude larger than the displacement \tilde{x} one wishes to measure. This apparently implies that our assumption is not justified.

The spread σ_x of the test particle's wave function could however be kept under control by using the loop protocol proposed in [8]. Specifically, through an appropriate alternation between an inverted harmonic potential and a harmonic one, the spatial probability distribution of a levitated nanoparticle is first expanded to scales much larger than the initial one and then converted back to the original configuration. Such a loop protocol works also in the presence of an external constant force F [8], like gravity (along x) in our case. In this way, the wave function of the test particle at $t = T$ can have the same spread as at $t = 0$, while being displaced by the gravitational

force F , as required to measure the effect we are after. We thus assume that this or a similar protocol ensuring $\sigma_x(T) = \sigma_x(0)$ is applied to the test particle B . This assumption is still quite optimistic at present, since the value $m_B = 10^{-14}$ kg we are assuming for the test mass is two orders of magnitude larger than the masses for which full quantum control has been achieved so far. We are however confident that progress will grant full quantum control for masses as large as 10^{-14} kg in the near future.

It should be noted, however, that ground-state cooling of the test mass m_B and preserving its spread during the experiment are not the main difficulties to be addressed in a practical implementation of our proposal. A major challenge is the preparation of a delocalized state for the required large values of the source mass m_A (of the order of 10^{-14} kg, at least) and separations d between the superposed locations (of the order of 10 μm). The state of the art is that separations of the order of a fraction of a micron have been achieved for macromolecules of several thousand of atoms, corresponding to masses of a fraction of 10^{-22} kg [35]. One sees that, for what we are proposing, experiments are off at present by several orders of magnitude in the mass and/or separation. It is however worth mentioning that experimental schemes for the preparation of masses approximately equal to 10^{-14} kg in a spatial quantum superposition state with an extent of the order of the micron have been proposed recently [36].

A further challenge is keeping quantum coherence for the quite long evolution times we are requiring here ($T \approx 1$ s). Coherence times of the order of 1 s have been shown for solid-state spin systems cooled down at 77 K [37] (coherence times become of the order 1 ms at room temperature [38]). For the kind of massive objects we are interested in, coherence times of the order of 1 s have been considered in the experimental scheme for the preparation of delocalized states just mentioned [36]. On the other hand, Ref. [39] has recently pointed out that, for massive objects, an intrinsic decoherence channel, which adds to decoherence from the environment, originates from the phonons within the object, which are almost unavoidably excited during the creation of the superposed state. A way to overcome this problem would be to make the applied force used to create the superposed state sufficiently homogeneous over the scale of the massive object, in order to minimize the creation of phonons. It is thus clear that both the preparation of the superposed state with the desired parameters and maintaining its quantum coherence for the required long times represent extremely difficult tasks, which will require a technological leap to be successfully addressed.

Returning to the discussion of Casimir-Polder effects, we notice that with the chosen value $\epsilon = 1$ μm for the distance between the two masses and the plate, Casimir-Polder forces by the plate on the two masses will be quite large, much larger, in particular, than the gravitational interaction between source and test masses. They will however have a vanishing component along x and thus will not spoil the measurement of the displacement along x of our interest. Actually, in the configuration of Fig. 3, Casimir-Polder forces could even be used to contrast the effects of earth's gravity on particle A (aiding, or altogether replacing, optical levitation). For particle B , a second plate could be arranged above it, parallel to

the first one at a distance less than ϵ in order to partially (or completely) balance earth's gravity. In the case of a good balance of the forces along the vertical (which might be achieved by adding also a third plate, this time below the delocalized particle A , to regulate the overall Casimir-Polder force on the latter) one would not have appreciable displacements Δy along y , even for times as large as $T \sim 1$ s (which would lead to $\Delta y \approx 5$ m for free fall). One could thus potentially perform the experiment in an earth-based laboratory with no need to go after free fall, use optical levitation, or envisage it as a space experiment.

In order to estimate the Casimir-Polder force F_{CP} between particles and plates, we can use its expression when the distance of closest approach to the plate is $l \leq r_{A,B}$,

$$F_{CP} = 2\pi r \left(\frac{1}{3} \frac{\pi^2 \hbar c}{240 l^3} \right), \quad (10)$$

where c is the speed of light in vacuum and r is the radius of the spherical masses [40]. Using this formula, one finds that, with $l = 0.3 \mu\text{m}$, F_{CP} alone is able to balance the weight of B , with no need of optical levitation. Indeed, for a silica spherical mass $m_B = 10^{-14}$ kg, one has $r_B = 0.97 \mu\text{m}$, yielding $F_{CP} = 0.98 \times 10^{-13}$ N $\approx m_B g$, where g is earth's gravity.

In comparison, the gravitational force F_{G-AB} between A and B is extremely feeble. From (8), with the same conditions discussed above (in particular, $m_A = 10^{-11}$ kg and $m_B = 10^{-14}$ kg), one gets $F_{G-AB} \approx 2.4 \times 10^{-26}$ N, which is about 13 orders of magnitude smaller than the Casimir-Polder forces. Such a huge difference makes it clear that, for the actual feasibility of the experiment, it is crucial to reach an extreme accuracy in the preparation of the setup. In particular, imperfections in the planarity of the metallic plate or in the spherical shape of the particles could produce side effects in the x direction that, even if much smaller than F_{CP} , could possibly overwhelm F_{G-ABx} or lead to variations of F_{CP} in the two superposed locations of the source particle that could spoil its coherence. Effects of this kind, possibly also changing with time, could originate from patch potentials and density fluctuations, as well as from any kind of irregularities of the surfaces.

Considering that our aim is to exploit Casimir-Polder forces rather than finding ways to suppress them, it is important to analyze this kind of effects, which could hinder the feasibility of the proposed experiment. For the source mass, the main issue could be a variation of the Casimir-Polder force between the mass and the plate in the two superposed locations due to the above random fluctuations. Previous studies [41,42] have shown that, for a sphere with radius R at an (average) distance l from the plate, with random corrugations of amplitude $\Delta z \ll l$ for both surfaces, the Casimir-Polder force does not depend on the position on the plate provided the characteristic lateral scales Λ_p and Λ_s for the surface roughness of the plate and the sphere, respectively, are small compared to \sqrt{Rl} (for $l \ll R$) or to l (for $R \ll l$; see [43]). With our numbers for the source mass ($R \approx 10 \mu\text{m}$ and $l \gtrsim 0.1 \mu\text{m}$), this would require keeping the amplitude Δz of the surface roughness within 10 nm and the lateral scales Λ_s and Λ_p within 100 nm. Under these conditions, the effect of the surface roughness would be just a correction by a multiplica-

tive factor [42] of the expression (10) for the force F_{CP} , with no variations between the two superposed positions and thus no spoiling of the delocalized state of the source mass.

Concerning electrostatic patch potentials, which could produce an electrostatic force on top of the Casimir-Polder force, a recent work [44] has shown that by applying an ion-blocking layer on the surfaces of the sphere and plate, the force produced by patches can be reduced to $10^{-4} F_{CP}$ for distances between the plate and the sphere of the same order as considered here. We speculate that such variations of the force, which could lead to an imperfect balance between the weight of the source mass and the Casimir-Polder force by the plate on top of it (see in particular the final experimental configuration described in the next section), could be eliminated by an optical levitation system with an effective potential conveniently shaped to compensate for the residual force difference (of order 10^{-4} the weight of the particle) between the two superposed locations.

For the test mass, the main issue could be the occurrence of lateral Casimir-Polder forces due to irregularities of the surface, which could produce a lateral displacement on top of the gravitational one. It should be pointed out, however, that for the same random short-scale irregularities just discussed, these forces cancel out altogether [42]. As a matter of fact, only parallel uniaxial sinusoidal corrugations of the surfaces with the same period can produce nonzero lateral Casimir-Polder forces, as also shown in the seminal experiment [45].

We notice here however that, even in the absence of such irregularities, the strong Casimir-Polder forces F_{CP} by the masses on the plate will likely deform it, with ensuing side effects possibly larger than those just mentioned. We thus focus on discussing these effects, which are present even for an ideal realization of the experimental setup.

Looking at Fig. 3, one can see that a deformation of the plate produced by F_{CP} when A is in one of the two branches, for example, when A is in R , gives an effective distance between B and the plate larger to the right than to the left and thus a Casimir-Polder attraction stronger towards the left than towards the right. One would thus have a Casimir-Polder acceleration along x , induced by the deformation, that is opposite to the one expected from gravitational interaction between A and B , possibly overwhelming it and thus undermining the experiment.

The deformation induced by a force F_{CP} acting at the center of a square plate of side ℓ and thickness s , with clamps at the ends at distance ℓ , say, along x , can be estimated as [46] (see also [25])

$$\delta_{\text{def}} = \frac{F_{CP} \ell^3}{192EI}, \quad (11)$$

where E is the Young modulus ($E = 137$ GPa if the plate is made of copper) and $I = \frac{\ell}{12} s^3$ is the area moment of the plate with respect to the axis through its center, parallel to the plate and orthogonal to the x direction. If F_{CP} corresponds to the weight of a particle of mass m (perfect balance), one has

$$\delta_{\text{def}} = mg \frac{\ell^2}{16Es^3}. \quad (12)$$

For $\ell = 1$ mm, $s = 1 \mu\text{m}$, and $m = 10^{-14}$ kg ($m = 10^{-11}$ kg) this gives $\delta_{\text{def}} = 0.45 \times 10^{-13}$ m ($\delta_{\text{def}} = 0.45 \times 10^{-10}$ m).

Strictly speaking, these deformations add to the deformation already present due the action of earth's gravity on the plate (which is symmetric about the plate center).

To estimate the effect of deformations of such an amount, let us compare F_{CP} corresponding to a given distance of closest approach $l \approx 0.1\text{--}10\ \mu\text{m}$ with the Casimir-Polder force F_{CP}^* one would get if this distance were larger by, say, $\eta = 10^{-13}\ \text{m}$, $l' = l + \eta$. One can roughly think that the left-right imbalance in the total Casimir-Polder force induced by the deformation should not be larger than the difference $F_{CP} - F_{CP}^*$. From Eq. (10) with $\eta \ll l$, one gets

$$F_{CP} - F_{CP}^* = 3\frac{\eta}{l}F_{CP}. \quad (13)$$

With $\eta = 10^{-13}\ \text{m}$ and the value $F_{CP} = 0.98 \times 10^{-13}\ \text{N}$ calculated above (corresponding to $l = 0.3\ \mu\text{m}$ and $r \approx 1\ \mu\text{m}$), one gets $F_{CP} - F_{CP}^* \approx 3 \times 10^{-20}\ \text{N}$, which is six orders of magnitude larger than the gravity force F_{G-AB} between $m_A = 10^{-11}\ \text{kg}$ and $m_B = 10^{-14}\ \text{kg}$.

This shows that to proceed with our program one should definitely address the issue of the induced deformations, including also the deformation of the plate under its own weight. The ideal solution would be keeping the deformations (at least the dangerous ones, i.e., those able to induce a left-right asymmetry along x at the actual position of B) small enough. In particular, for deformations smaller than the zero-point motion δ_0 of the plate considered as a harmonic oscillator, one expects the oscillator to relax to the ground state with no significant effect from the (would be) deformation.

To estimate the zero-point motion of the center of the plate, we describe it as a harmonic oscillator with mass M equal to the mass of the plate, elastic constant $k = \frac{16E_s^3}{l^2}$ [in view of Eq. (11) written as $\delta_{\text{def}} = \frac{F_{CP}}{k}$], and angular frequency $\omega = \sqrt{\frac{k}{M}}$ [25]. Analogously to Eq. (9), the zero-point motion along y of the center of the plate can be estimated as

$$\delta_0 = \sqrt{\frac{\hbar}{2M\omega}} = \sqrt{\frac{\hbar}{2\sqrt{Mk}}} = \frac{1}{2\sqrt{2}s} \sqrt{\frac{\hbar}{\rho E}}, \quad (14)$$

where ρ is the density of the material the plate is made of. For copper ($\rho = 8.96 \times 10^3\ \text{kg/m}^3$) and taking $s = 1\ \mu\text{m}$, one gets $\delta_0 = 0.61 \times 10^{-15}\ \text{m}$.

Actually, the ground-state oscillations of the plate alone might in principle overwhelm the effects we are after. Indeed, the zero-point motion deviation δ of the plate from its equilibrium position varies along the distance connecting the clamps, being $\delta = \delta_0$ maximal in the middle and $\delta \approx 0$ at the clamps, thus inducing a gradient along x of the Casimir force. An upper bound for the effects of the possible ground-state motion asymmetry is provided by replacing η with δ_0 in Eq. (13), yielding $F_{CP} - F_{CP}^* \approx 10^{-22}\ \text{N}$, which is four orders of magnitude larger than the gravity force F_{G-AB} calculated above. This means that the ground-state oscillations of the plate alone might in principle overwhelm the effects we are after.

The aim of the following section is thus to modify the setup of Fig. 3 and find a configuration that overcomes the problems due to ground-state motion, to the deformations induced by

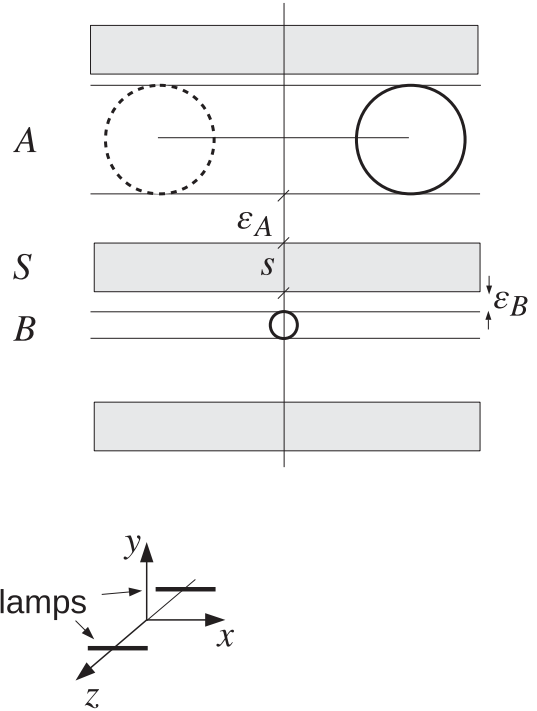


FIG. 4. Proposed experimental setup. The metallic plate S screens the Casimir-Polder forces between the two particles and partially or fully compensates the weight of B with Casimir-Polder forces. The additional plate on top of A partially or fully compensates the weight of A , while the optional plate below B can be used for a fine-tuning of the levitation of B . The clamps for the plates are separated by a distance ℓ along z .

the test and source masses, and to the deformation of the plate by its own weight.

IV. OUR PROPOSAL

Our proposal is based on adjusting the parameters and the spatial arrangement of masses and plates and on taking advantage as much as possible of symmetry considerations, in order to minimize adverse effects.

First of all, the Casimir-Polder force balancing the weight of the delocalized mass A should not act on the plate separating A and B (as in Fig. 3). We saw indeed that a deformation-induced left-right imbalance in the Casimir-Polder force by the separating plate on B could overwhelm the gravitational effects between A and B .

We thus propose to place A above the plate S separating the two masses and add above A a second plate, as shown in Fig. 4. This second plate, if sufficiently close to A , could balance the weight of A through Casimir-Polder forces. At the same time, deformations of this plate by the mass A will not affect the superposition of states of A , since the effects of deformations will be identical in the two branches. The separation between A and S can then be chosen as large as required for keeping the Casimir-Polder deformation of S below the ground-state oscillation of the plate.

The test mass B can be placed close to S to compensate its weight with the Casimir-Polder force of S (aiding, or even completely replacing, optical levitation). The deformation in-

duced by B on S , even if somehow larger than the ground-state motion of the plate, is not an issue because it is completely symmetric with respect to the position of B and thus expected to have no Casimir-Polder effect on the motion of B along x . One might however possibly expect some higher-order effects if B is not exactly centered with respect to the clamps.

These potential effects, as well as the deformation of the plate S under its own weight, and the effects due to its ground-state motion can all be taken to be reasonably under control if the clamps on S are put at a distance ℓ along the direction z (orthogonal to x , in the plane; see Fig. 4). Indeed, with this choice, all of these deformations vary only along z and should not produce any effect along x .

A third plate could finally be arranged below B (see Fig. 4) to allow for fine adjustments to get an exact balance of the weight of B (in the absence of optical levitation, in particular).

We now proceed to estimate the value of the distance ϵ_A required to keep the deformation induced by A below the ground-state motion of S . To this end, we notice that Eq. (14), for a value $s = 2 \mu\text{m}$ of the thickness of S , yields the value $\delta_0 \approx 0.3 \times 10^{-15} \text{ m}$ for the ground-state motion of the center of the plate (which is the same for all points along x in the middle of the plate). On the other hand, a choice of $\epsilon_A = 3 \mu\text{m}$ yields for the deformation δ_{def} (Casimir-Polder) induced by A on S the value $\delta_{\text{def}} \approx 0.6 \times 10^{-16} \text{ m}$, as obtained by inserting $l = \epsilon_A$ in Eq. (11), with F_{CP} given by Eq. (10). Here we are considering a square plate of copper with side length $\ell = 1 \text{ mm}$. This value of ϵ_A thus guarantees $\delta_{\text{def}} \ll \delta_0$, and no effects are expected from possible deformations induced by A .

V. EXPECTED SIGNAL

We can now proceed to estimate the displacements \tilde{x} of B along x produced by the gravitational field sourced by A in each of the two branches.

The displacement can be conveniently written as a function of the mass m_A of the delocalized particle and of the evolution time T , $\tilde{x} = \tilde{x}(m_A, T)$, as

$$\tilde{x} = \frac{1}{2} a_x T^2 \quad (15)$$

$$= \frac{1}{3\sqrt{3}} \frac{Gm_A}{\tilde{y}_B^2} T^2 \quad (16)$$

$$= \frac{1}{3\sqrt{3}} \frac{Gm_A}{\left[\left(\frac{3}{4\pi}\right)^{1/3} \left(\frac{m_A}{\rho}\right)^{1/3} + \tilde{y}_B\right]^2} T^2, \quad (17)$$

where $\rho = 2.6 \times 10^3 \text{ kg/m}^3$ for silica and $\tilde{y}_B \equiv r_B + \epsilon_B + s + \epsilon_A = 6.3 \mu\text{m}$ (for fixed $m_B = 10^{-14} \text{ kg}$). In Eq. (16) we have assumed that d is optimal (namely, the choice that maximizes a_x , as described above). For the above value $\tilde{y}_B \approx 6 \mu\text{m}$, the geometrical constraint $d/2 > r_A$ is respected for masses $m_A \lesssim 4 \times 10^{-11} \text{ kg}$. The distance $d/2$ varies from $5.1 \mu\text{m}$ to $11.3 \mu\text{m}$ as m_A changes from 10^{-14} kg to 10^{-11} kg (and r_A varies correspondingly from $0.97 \mu\text{m}$ to $9.7 \mu\text{m}$).

Figure 5 shows the displacement \tilde{x} as a function of the mass m_A of the delocalized particle assuming an evolution time $T = 1 \text{ s}$ and a mass $m_B = 10^{-14} \text{ kg}$ for the test particle which, according to (9), gives a spatial resolution better than 0.1 pm . One sees from Fig. 5 that the displacement should in principle be detectable for a source mass $m_A \gtrsim 10^{-12} \text{ kg}$.

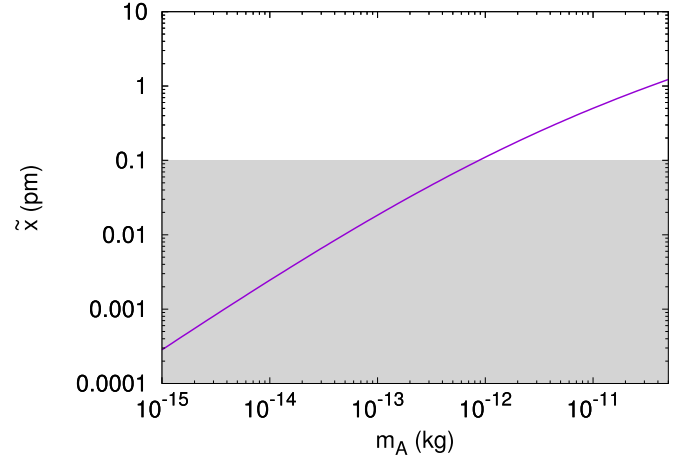


FIG. 5. Displacement \tilde{x} of the test mass $m_B = 10^{-14} \text{ kg}$, after a time $T = 1 \text{ s}$, as a function of the mass m_A of the delocalized source particle. The shaded area shows the displacement below the current resolution limit (0.1 pm). Test and source masses are assumed to be made of silica.

This lower bound for the source mass m_A could be reduced for evolution times longer than $T = 1 \text{ s}$. This is shown in Fig. 6, which displays the displacement \tilde{x} as a function of the evolution time for different values of the delocalized source mass m_A . Displacement would exceed the spatial resolution of 0.1 pm and be detectable outside the shaded area in Fig. 6.

As already mentioned, maintaining coherence on timescales $T \gtrsim 1 \text{ s}$ for masses $m_A \approx 10^{-14}$ is clearly not an easy task. The system has to be cooled down to very low temperatures since thermal photons alone are able to wash out coherence very rapidly, no matter how good the vacuum is in the experimental setup [34]. Experimental schemes able to reach the above timescales for masses approximately equal to 10^{-14} kg and separations of the order of their size have been proposed in [36]. They require temperatures of a few

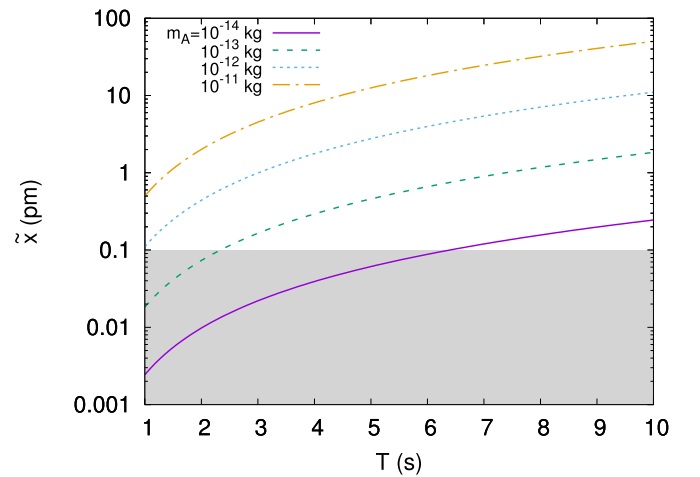


FIG. 6. Displacement \tilde{x} of a silica test mass $m_B = 10^{-14} \text{ kg}$ as a function of the evolution time T , for different values of the delocalized source mass m_A . The shaded area shows the displacement below the current resolution limit (0.1 pm). Test and source masses are assumed to be made of silica.

tens of mK at most and pressures at the state-of-the-art level of $P \approx 10^{-20}$ bar.

VI. CONCLUSION

In summary, we have described a possible setup in a laboratory setting to check for the quantum nature of the gravitational field. This was done by exploiting the ability of the gravitational field to become entangled with the superposed positions of a single delocalized particle, if the field is quantum in nature.

In a way, our proposal can be regarded as an attempt to turn part of the gedanken experiment of [47–53] (where a test particle probes the gravitational field of a delocalized particle while this recombines) into something real. Specifically, it is an attempt for a practical implementation of the which-path part of the gedanken experiment, consisting in the ability of the test particle to discriminate which branch is taken in the superposition, if the field requires a quantum description.

To turn the thought experiment into something real, we have shown that the test particle should be placed very close to the delocalized one, thus potentially clashing with Casimir-Polder effects, which are expected to overwhelm the signal we are after. We discussed a way to overcome this difficulty, basically using electrical screening through metallic plates, as conceived also, for different settings, in [9,25,26]. In the setup we have considered, it turns out that Casimir-Polder forces can actually be used, instead of simply be fought, to help in balancing the weight of the particles (possibly eliminating altogether the need of optical levitation).

The proposed setup requires a good enough sensitivity to the displacement of the test particle, which, if gravity is quantum, is differential in the two superposed branches. This involves the use of delocalized particles with masses greater than approximately 10^{-14} kg and separations approximately equal to 10–20 μm , which should keep quantum coherence for time intervals as long as 1–10 s. These requirements are

not so different from other proposals for gravity-induced entanglement experiments [15,25], but, as mentioned, remain extremely challenging at present. Innovative techniques to prepare such large masses in a delocalized state with such large separations have crucially to be envisaged [36], including severe cooling of the system ($T \lesssim 10$ mK) and extremely low pressures ($P \lesssim 10^{-20}$ bar) to keep control on its evolution. As for the test particle, the needed spatial resolution with optical tweezers through ground-state cooling requires masses greater than approximately 10^{-14} kg, two orders of magnitude larger than the largest mass controlled so far with these techniques. Finally, even if our investigation has been only at a proof-of-concept level, we have discussed that possible imperfections in the components of the experimental apparatus, in particular concerning the accuracy of the planarity of the metallic screens and random irregularities of the surfaces could critically affect the feasibility of the experiment and deserve careful consideration. In this respect, we have argued that by keeping the lateral scale for the surface roughness within 100 nm and the amplitude of fluctuations within 10 nm, the effects of irregularities could be kept under control. Ion-blocking layers applied to the surfaces and a fine-tuning of the balance between the Casimir-Polder force and the weight provided by an additional optical levitation system could finally eliminate also disturbances originating by electromagnetic patch potentials.

We hope that all of these challenges, apparently more technical than fundamental in nature, might be successfully addressed in future experiments.

ACKNOWLEDGMENTS

We thank Alessio Belenchia, Sumanta Chakraborty, Dawood Kothawala, Lorenzo Piroli, Massimiliano Rossi, Valerio Scarani, and Peter Sidajaya for reading the manuscript and/or discussions. Partial financial support from INFN through grants FLAG and QUANTUM is acknowledged.

-
- [1] D. Carney, P. C. E. Stamp, and J. M. Taylor, Tabletop experiments for quantum gravity: A user's manual, *Class. Quantum Grav.* **36**, 034001 (2019).
 - [2] N. Huggett, N. Linnemann, and M. D. Schneider, *Quantum Gravity in a Laboratory?* (Cambridge University Press, Cambridge, 2023).
 - [3] R. P. Feynman, in *The Role of Gravitation in Physics: Report from the 1957 Chapel Hill Conference*, edited by C. M. DeWitt and D. Rickles (Max Planck Research Library for the History and Development of Knowledge, Berlin, 2011).
 - [4] C. Møller, in *Proceedings, Les Théories Relativistes de la Gravitation: Actes du Colloques Internationaux, Royaumont, 1959*, edited by A. Lichnerowicz and M.-A. Tonnelat (CNRS, Paris, 1962), Vol. 91, p. 15.
 - [5] L. Rosenfeld, On quantization of fields, *Nucl. Phys.* **40**, 353 (1963).
 - [6] M. Aspelmeyer, in *From Quantum to Classical: Essays in Honour of H.-Dieter Zeh*, edited by C. Kiefer, *Fundamental Theories of Physics* Vol. 204 (Springer, Cham, 2022).
 - [7] P. Sidajaya, W. Cong, and V. Scarani, Possibility of detecting gravity of an object frozen in a spatial superposition by the Zeno effect, *Phys. Rev. A* **106**, 042217 (2022).
 - [8] T. Weiss, M. Roda-Llorges, E. Torrontegui, M. Aspelmeyer, and O. Romero-Isart, Large quantum delocalization of a levitated nanoparticle using optimal control: Applications for force sensing and entangling via weak forces, *Phys. Rev. Lett.* **127**, 023601 (2021).
 - [9] T. Westphal, H. Hepach, J. Pfaff, and M. Aspelmeyer, Measurement of gravitational coupling between millimetre-sized masses, *Nature (London)* **591**, 225 (2021).
 - [10] N. H. Lindner and A. Peres, Testing quantum superpositions of the gravitational field with Bose-Einstein condensates, *Phys. Rev. A* **71**, 024101 (2005).
 - [11] M. Derakhshani, C. Anastopoulos, and B. L. Hu, Probing a gravitational cat state: Experimental possibilities, *J. Phys.: Conf. Ser.* **701**, 012015 (2016).
 - [12] M. Carlesso, M. Paternostro, H. Ulbricht, and A. Bassi, When Cavendish meets Feynman: A quantum torsion balance for testing the quantumness of gravity, [arXiv:1710.08695](https://arxiv.org/abs/1710.08695).

- [13] M. Carlesso, A. Bassi, M. Paternostro, and H. Ulbricht, Testing the gravitational field generated by a quantum superposition, *New J. Phys.* **21**, 093052 (2019).
- [14] S. Bose, Matter wave Ramsey interferometry & the quantum nature of gravity (2016), available at https://www.youtube.com/watch?v=0Fv-0k13s_k.
- [15] S. Bose, A. Mazumdar, G. W. Morley, H. Ulbricht, M. Toroš, M. Paternostro, A. A. Geraci, P. F. Barker, M. S. Kim, and G. Milburn, A spin entanglement witness for quantum gravity, *Phys. Rev. Lett.* **119**, 240401 (2017).
- [16] C. Marletto and V. Vedral, Gravitationally-induced entanglement between two massive particles is sufficient evidence of quantum effects in gravity, *Phys. Rev. Lett.* **119**, 240402 (2017).
- [17] A. Al Balushi, W. Cong, and R. B. Mann, An optomechanical quantum Cavendish experiment, *Phys. Rev. A* **98**, 043811 (2018).
- [18] T. Krisnanda, G. Y. Tham, M. Paternostro, and T. Paterek, Observable quantum entanglement due to gravity, *npj Quantum Inf.* **6**, 12 (2020).
- [19] R. J. Marshman, A. Mazumdar, and S. Bose, Locality and entanglement in table-top testing of the quantum nature of linearized gravity, *Phys. Rev. A* **101**, 052110 (2020).
- [20] R. Howl, V. Vedral, D. Naik, M. Christodoulou, C. Rovelli, and A. Iyer, Non-Gaussianity as a signature of a quantum theory of gravity, *PRX Quantum* **2**, 010325 (2021).
- [21] L. Lami, J. S. Pedernales, and M. B. Plenio, Testing the quantum nature of gravity without entanglement, [arXiv:2302.03075](https://arxiv.org/abs/2302.03075).
- [22] H. B. G. Casimir, On the attraction between two perfectly conducting plates, *Kon. Ned. Akad. Wetensch. Proc.* **51**, 793 (1948).
- [23] H. B. G. Casimir and D. Polder, The influence of retardation on the London–van der Waals forces, *Phys. Rev.* **73**, 360 (1948).
- [24] E. A. Power, Casimir-Polder potential from first principles, *Eur. J. Phys.* **22**, 453 (2001).
- [25] T. W. van de Kamp, R. J. Marshman, S. Bose, and A. Mazumdar, Quantum gravity witness via entanglement of masses: Casimir screening, *Phys. Rev. A* **102**, 062807 (2020).
- [26] B. Yi, U. Sinha, D. Home, A. Mazumdar, and S. Bose, Spatial qubit entanglement witness for quantum natured gravity, [arXiv:2211.03661](https://arxiv.org/abs/2211.03661).
- [27] O. Romero-Isart, Quantum superposition of massive objects and collapse models, *Phys. Rev. A* **84**, 052121 (2011).
- [28] F. Tebbenjohanns, M. Frimmer, A. Militarú, V. Jain, and L. Novotny, Cold damping of an optically levitated nanoparticle to microkelvin temperatures, *Phys. Rev. Lett.* **122**, 223601 (2019).
- [29] U. Delić, M. Reisenbauer, K. Dare, D. Grass, V. Vuletić, N. Kiesel, and M. Aspelmeyer, Cooling of a levitated nanoparticle to the motional quantum ground state, *Science* **367**, 892 (2020).
- [30] J. S. Pedernales, K. Streltsov, and M. B. Plenio, Enhancing gravitational interaction between quantum systems by a massive mediator, *Phys. Rev. Lett.* **128**, 110401 (2022).
- [31] F. Tebbenjohanns, M. L. Mattana, M. Rossi, M. Frimmer, and L. Novotny, Quantum control of a nanoparticle optically levitated in cryogenic free space, *Nature (London)* **595**, 378 (2021).
- [32] S. Gasiorowicz, *Quantum Physics* (Wiley, Singapore, 1974).
- [33] V. B. Braginsky, Y. I. Vorontsov, and K. S. Thorne, Quantum nondemolition measurements, *Science* **209**, 547 (1980).
- [34] E. Joos, H. D. Zeh, C. Kiefer, D. Giulini, J. Kupsch, and I.-O. Stamatescu, *Decoherence and the Appearance of a Classical World in Quantum Theory* (Springer, Berlin, 2003).
- [35] Y. Y. Fein, P. Geyer, P. Zwick, F. Kiałka, S. Pedalino, M. Mayor, S. Gerlich, and M. Arndt, Quantum superposition of molecules beyond 25 kDa, *Nat. Phys.* **15**, 1242 (2019).
- [36] H. Pino, J. Prat-Camps, K. Sinha, B. P. Venkatesh, and O. Romero-Isart, On-chip quantum interference of a superconducting microsphere, *Quantum Sci. Technol.* **3**, 025001 (2018).
- [37] N. Bar-Gill, L. M. Pham, A. Jarmola, D. Budker, and R. L. Walsworth, Solid-state electronic spin coherence time approaching one second, *Nat. Commun.* **4**, 1743 (2013).
- [38] E. D. Herbschleb, H. Kato, Y. Maruyama, T. Danjo, T. Makino, S. Yamasaki, I. Ohki, K. Hayashi, H. Morishita, M. Fujiwara, and N. Mizuochi, Ultra-long coherence times amongst room-temperature solid-state spins, *Nat. Commun.* **10**, 3766 (2019).
- [39] C. Henkel and R. Folman, Universal limit on spatial quantum superpositions with massive objects due to phonons, [arXiv:2305.15230](https://arxiv.org/abs/2305.15230).
- [40] S. K. Lamoreaux, Demonstration of the Casimir force in the 0.6 to 6 μm range, *Phys. Rev. Lett.* **78**, 5 (1997).
- [41] G. L. Klimchitskaya and Y. V. Pavlov, The corrections to the Casimir forces for configurations used in experiments: The spherical lens above the plane and two crossed cylinders, *Int. J. Mod. Phys. A* **11**, 3723 (1996).
- [42] G. L. Klimchitskaya, U. Mohideen, and V. M. Mostepanenko, The Casimir force between real materials: Experiment and theory, *Rev. Mod. Phys.* **81**, 1827 (2009).
- [43] V. B. Bezerra, G. L. Klimchitskaya, and C. Romero, Surface roughness contribution to the Casimir interaction between an isolated atom and a cavity wall, *Phys. Rev. A* **61**, 022115 (2000).
- [44] J. L. Garrett, J. Kim, and J. N. Munday, Measuring the effect of electrostatic patch potentials in Casimir force experiments, *Phys. Rev. Res.* **2**, 023355 (2020).
- [45] F. Chen, U. Mohideen, G. L. Klimchitskaya, and V. M. Mostepanenko, Demonstration of the lateral Casimir force, *Phys. Rev. Lett.* **88**, 101801 (2002).
- [46] L. D. Landau and E. M. Lifshitz, *Theory of Elasticity*, 3rd ed. (Pergamon, Oxford, 1986).
- [47] G. Baym and T. Ozawa, Two-slit diffraction with highly charged particles: Niels Bohr’s consistency argument that the electromagnetic field must be quantized, *Proc. Natl. Acad. Sci. USA* **106**, 3035 (2009).
- [48] A. Mari, G. De Palma, and V. Giovannetti, Experiments testing macroscopic quantum superpositions must be slow, *Sci. Rep.* **6**, 22777 (2016).
- [49] A. Belenchia, R. M. Wald, F. Giacomini, E. Castro-Ruiz, Č. Brukner, and M. Aspelmeyer, Quantum superposition of massive objects and the quantization of gravity, *Phys. Rev. D* **98**, 126009 (2018).
- [50] A. Belenchia, R. M. Wald, F. Giacomini, E. Castro-Ruiz, Č. Brukner, and M. Aspelmeyer, Information content of the gravitational field of a quantum superposition, *Int. J. Mod. Phys. D* **28**, 1943001 (2019).
- [51] E. Rydving, E. Aurell, and I. Pikovski, Do Gedanken experiments compel quantization of gravity?, *Phys. Rev. D* **104**, 086024 (2021).
- [52] D. L. Danielson, G. Satishchandran, and R. M. Wald, Gravitationally mediated entanglement: Newtonian field versus gravitons, *Phys. Rev. D* **105**, 086001 (2022).
- [53] A. Pesci, Conditions for graviton emission in the recombination of a delocalized mass, *Quantum Rep.* **5**, 426 (2023).